Parameter Identification of Tram Acoustic Models for Noise Mapping from Pass-by Measurements

Olivier Chiello, Annabelle Caura, Marie Agnès Pallas

PARAMETER IDENTIFICATION OF TRAM ACOUSTIC MODELS FOR NOISE MAPPING FROM PASS-BY MEASUREMENTS

Olivier Chiello[1] **Annabelle Caura**[1] **Marie-Agnès Pallas**[1]
[1] UMRAE, Univ Gustave Eiffel, IFSTTAR, CEREMA, Univ Lyon, F-69675, Lyon, France
olivier.chiello@univ-eiffel.fr

ABSTRACT

From the beginning of 2019, the new European common method CNOSSOS-EU must be used for strategic noise mapping in accordance with Directive 2002/49/EC. For the assessment of railway noise emissions, the method requires a detailed description level. Firstly, the contributions of the different sources (rolling, traction) must be specified. Furthermore, for rolling noise, excitation data (wheel/rail roughness) must be distinguished from the vibro-acoustic efficiency (track/vehicle transfer functions) as well as the respective contributions of track and vehicle. For conventional railways, national operators generally have a large amount of experimental data and models available to evaluate these input parameters. This is not the case for tramway networks, for which few studies or measurements exist, particularly with regard to wheel and rail roughness or track transfer functions. This study aims to identify the parameters required by CNOSSOS-EU, based on pass-by and wheel/rail roughness measurements for several sites and vehicles on the Lyon tramway network. Near-field emission and propagation models are first developed and then, an inverse method is proposed for parameter identification. The data obtained are compared with the default values of the CNOSSOS method for conventional rail.

1. INTRODUCTION

The European Directive 2002/49/EC [1] makes it compulsory for Member States to create noise maps in order to assess people's exposure to noise. These maps are made available to the public and allow the implementation of action plans to reduce noise. Their production is mandatory for large urban areas as well as major road and rail transport routes, airports and industrial sites. A common method, called CNOSSOS-EU for Common Noise Assessment Methods in Europe [2] was published in 2015 to harmonise the production of noise maps between all EU countries.

The CNOSSOS-EU procedure for the calculation of emission terms corresponding to railway noise is very detailed. First of all, the different sources of railway noise (rolling noise, traction noise and aerodynamic noise) must be distinguished: the corresponding sound powers must be specified in the model. In addition, the rolling noise term must be estimated from the specific contributions of the vehicle and the track, themselves calculated from wheel/rail roughness and transfer functions characterizing the track and the vehicle vibro-acoustic efficiency (see Fig. 1).

In its appendix, the method gives a series of tabulated values, corresponding to conventional vehicles or tracks. Moreover, major national operators generally have experimental data or advanced models at their disposal to evaluate these new input parameters for their rolling stock. This is generally not the case for tram networks, for which very few measurements exist, notably concerning the wheel and rail roughness or the transfer functions. With regard to rail roughness, some measurements show significant differences with conventional rail [3–7]. Concerning the separation of noise sources and the contributions of track and vehicle to rolling noise, existing models also show that tramways have their own properties [6, 8–15].

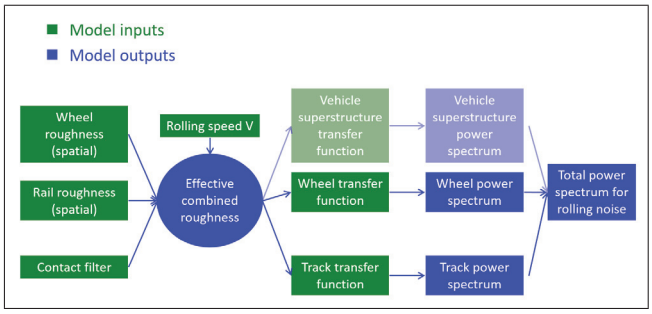

Figure 1. CNOSSOS rolling noise model.

This paper investigates an empirical approach identifying some of the main acoustic parameters of the CNOSSOS-EU model through simple measurements on a tram network. It consists in estimating both the traction noise spectrum and the rolling noise transfer function from pass-by noise levels and roughness measurements. The separation of wheel/track contributions [1] to the transfer function is not addressed here and will be considered in a second stage. The method is based on the inversion of specific emission and propagation models adapted to the assessment of equivalent pass-by noise levels. After a brief description and analysis of the available measurements, the identification method is presented. The assumptions of the different models are detailed as well as the inversion approach implemented. The results are then presented and the performance of the proposed method is examined. Finally, the realism and accuracy of the model are discussed,

[1] The vehicle superstructure only concerns freight wagons and is irrelevant here.

in particular concerning the effect of speed on emission levels.

2. AVAILABLE MEASUREMENTS

Pass-by measurements used to test the identification method were carried out in 2018 by the association Acoucité, on part of the Lyon tramway network. The equivalent pressure level, averaged over pass-by time, was measured according to standard ISO 3095:2013 as three types of vehicles ran at various speeds, over four different track sections. They are trainsets of the commercial schedule passing-by at the experimentation time. Two microphones were used, both placed 7.5 m from the track centreline, the lower one at a height of 1.2 m as specified in the standard ISO 3095, and the upper one at 3.5 m. The results corresponding to only one vehicle type are presented in this paper. All train-sets of this type are 27 m long and 3.68 m high. They are composed of two units separated by a carrier basket, all resting on three bogies (see Fig. 5). The two extreme bogies are motorised bogies equipped with disc-braked resilient wheels with a diameter of 72 mm. The central bogie is a carrying bogie equipped with disc-braked resilient wheels with a diameter of 65 cm. Measurements were performed on four track sections corresponding to different rails, track supports and surfacing. Two tracks have grooved rails and track laying with bi-block sleepers, embedded in a concrete slab (sections A and B). The other two tracks are equipped with Vignole rails laying on monobloc concrete sleepers and ballast (sections C and D). Sections B and C are characterized by the addition of a grassy coating, outcropping the rail head. Section B is also characterized by a slight curve, unlike the three others that are located on straight lines.

Fig. 2 shows the equivalent pressure level at pass-by as a function of speed V in logarithmic scale, for all the measurements carried out on the four sites. Quite different behaviours can be observed depending on the site, highlighted by the calculation of a linear regression of noise levels in $\alpha \log V$. In particular, site A is characterized by a very low slope α, probably due to the fact that only low speed pass-bys were recorded over a limited speed range. The spectra in third of octave bands corresponding to each pass-by are also available but are not shown here.

Wheel/rail roughness was also measured according to standard EN 15610:2018 as detailed in [7]. Wheel roughness measurements were carried out in workshop on free wheels. Wheels of three vehicles with different mileages since the last reprofiling were examined. Rail roughness measurements were carried out on both rails of each track section, for various lateral positions on the railhead. The final results obtained, in terms of mean rail roughness spectra corresponding to each section, as well as wheel roughness spectrum averaged over the three vehicles are given in Fig. 3. These data are used as input parameters in the identification method presented in the next section.

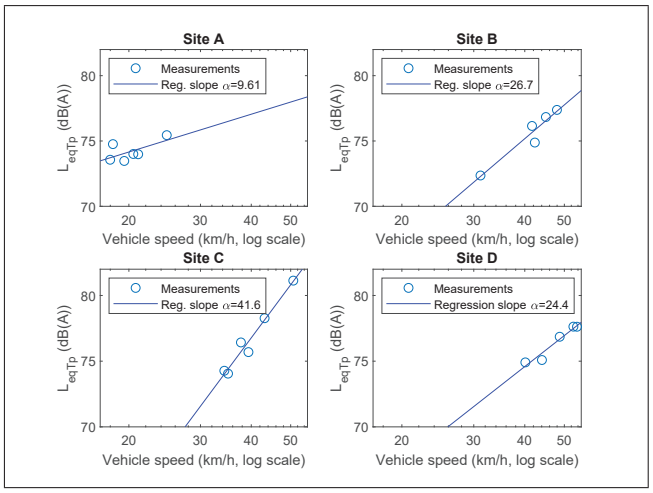

Figure 2. Global equivalent pass-by noise levels as a function of tram speed for all pass-bys (lower microphone)

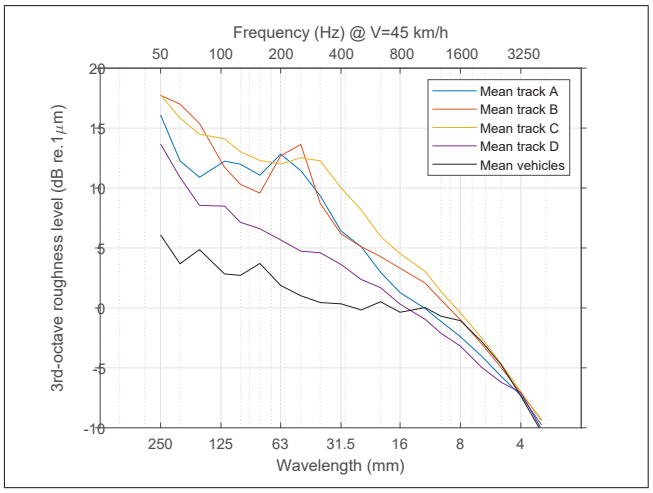

Figure 3. Wheel and rail roughness spectra as a function of wavelength (resp. frequency at 45 km/h)

3. IDENTIFICATION METHOD

The objective of the identification method is to empirically estimate both the traction power spectrum and the transfer function corresponding to the rolling noise from the measured pass-by noise and roughness spectra presented in the previous section. Traction noise emission is supposed to be independent of the site and constant with speed (in accordance with CNOSSOS-EU). It includes all contributions from propulsion and other onboard equipment. In the present approach, site-specific transfer functions are to be determined since the separation of wheel/track contributions is not considered in this first step. The method is based on the inversion of a whole emission/propagation model allowing the assessment of pass-by noise levels from the parameters to be identified (see Fig. 4).

3.1 Emission model

For this purpose, each pass-by is modelled by a combination of several moving point sources, located at different positions on the vehicle (see Fig. 5) :

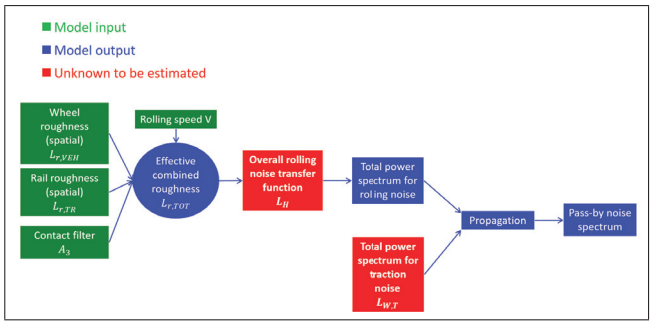

Figure 4. Emission/propagation model for the inversion method

- n_R sources $s \in \mathcal{S}_R$, corresponding to the wheel/rail rolling noise, located at height $h_l = 0.5$ m and centered on each wheelset,
- n_{Tl} sources $s \in \mathcal{S}_{Tl}$, corresponding to the traction noise due to motorised bogies, located at height $h_l = 0.5$ m and centered on motorised bogies,
- n_{Th} sources $s \in \mathcal{S}_{Th}$, corresponding to other potential traction noise including equipment like air-conditioning systems, located at height $h_h = 4$ m and regularly distributed along the vehicle.

Due to the low speed range considered, aerodynamic noise is not taken into account. Other specific sources like squeal noise, impact noise or bridge noise are out of scope, since not occurring on the measurement sites. The two source heights correspond to the CNOSSOS-EU model whereas the source distribution along the vehicle is fixed according to physical considerations. It should be noted, however, that the precision of the longitudinal distribution has only a limited effect on the pass-by noise level. No detailed information was available on the location of potential high sources of traction noise. The placement of these sources is optimised to be equivalent to an uniform line source model of finite length (vehicle length L) for the calculation of the pass-by pressure levels at 7.5 m.

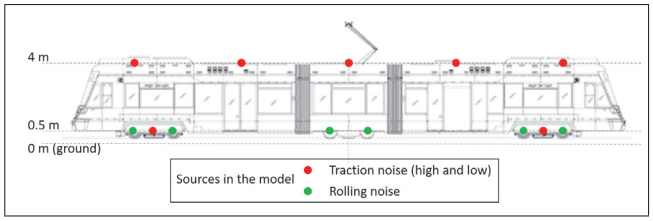

Figure 5. Location of point sources in the emission model.

The sound powers of the sources are determined using the following equations, in accordance with the CNOSSOS procedure for the calculation of rolling noise. The variation with the frequency band is implicit.

$$\begin{aligned} L_{W,s} &= L_H + L_{r,\mathrm{TOT}} \quad \forall s \in \mathcal{S}_R \\ L_{W,s} &= L_{W,T} + 10\log \alpha_l/n_{Tl} \quad \forall s \in \mathcal{S}_{Tl} \\ L_{W,s} &= L_{W,T} + 10\log \alpha_h/n_{Th} \quad \forall s \in \mathcal{S}_{Th} \end{aligned} \tag{1}$$

where L_H denotes the total transfer function corresponding to rolling noise and $L_{W,T}$ represents the whole sound power of the trainset corresponding to traction noise. Both parameters L_H and $L_{W,T}$ have to be identified. $L_{r,\mathrm{TOT}}$ represents the effective combined roughness such that :

$$L_{r,\mathrm{TOT}} = 10\log\left(10^{L_{r,\mathrm{VEH}}/10} + 10^{L_{r,\mathrm{TR}}/10}\right) + A_3 \tag{2}$$

where $L_{r,\mathrm{VEH}}$ and $L_{r,\mathrm{TR}}$ are the measured roughness power spectra corresponding respectively to wheels and rails, expressed as a function of frequency f for a given vehicle speed V using relation $f = V/\lambda$. A linear interpolation method is applied to obtain the roughness in the standard third of octave frequency bands from measurements given in Fig. 3, in accordance with the CNOSSOS-EU method. Transfer function A_3 is the contact filter, also expressed as a function of frequency, calculated here from an interpolation of the values proposed in CNOSSOS-EU in order to correspond to the tram wheel diameters and load. The constants α_l and $\alpha_h = 1-\alpha_l$ characterize the relative distribution of the traction noise on low and high sources. Among the various options tested, the distribution $\alpha_l = \alpha_l = 0.5$ lead to the best results and is considered in the following of the paper.

3.2 Propagation model

For the calculation of the propagation from source to receiver, the vehicle is first considered to be fixed, centered at a distance x from the track point located in front of the receiver. For each source s, the pressure level $L_{p,s}$ at the receiver point is calculated from the source power $L_{W,s}$ using the following formula:

$$L_{p,s}(x) = L_{W,s} + \Delta L_{W,\mathrm{dir},s}(x) - A_s(x) \tag{3}$$

where $\Delta L_{W,\mathrm{dir},s}$ is the attenuation due to directivity, depending on the horizontal and vertical angles (θ_s, Φ_s) denoting the relative position of the source with respect to the receiver, and on the centre frequency of each frequency band, whereas $A_s = A_{\mathrm{div,s}} + A_{\mathrm{atm,s}} + A_{\mathrm{ground,s}}$ is a global attenuation term, including :

- the attenuation due to geometrical divergence $A_{div,s} = 10\log 4\pi r_s^2$, depending on the distance r_s from the source to the receiver,
- the attenuation due to atmospheric absorption $A_{atm,s} = \alpha_{atm} r_s/1000$, where α_{atm} is the atmospheric attenuation coefficient depending of centre frequency of each frequency band, in accordance with ISO 9613-1,
- the attenuation due to ground effect $A_{ground,s}$ depending on geometrical parameters, acoustic wavenumber and ground impedance.

These directivity and attenuation terms implicitely include the actual individual source location according to the trainset position x. The directivity patterns used are those defined in the CNOSSOS-EU model and are different for

lower and upper sources. Considering the specificities of the actual propagation problem (homogeneous ground, receiver close to the track), the attenuation due to ground effect is not determined using the CNOSSOS-EU model but with a more accurate method, taking account of the expression of the spherical reflection coefficient as a function of the ground impedance Z, as provided for instance by Bérengier *et al.* [16]. The calculation of the impedance Z is carried out with the simple Delany-Bazley model [17] which only depends on the flow resistivity of the ground σ. The following values are chosen according to the site:

- site A (concrete) , $\sigma = 3 \times 10^7$ Pa.s.m^{-2},
- site B and C (grass) , $\sigma = 2 \times 10^5$ Pa.s.m^{-2},
- site D (ballast) , $\sigma = 5 \times 10^4$ Pa.s.m^{-2}.

3.3 Pass-by noise levels

Considering all noise sources included in the model, the equivalent pressure level at pass-by $L_{eq,Tp}$ is obtained by using a quasi-static assumption, e.g. neglecting Doppler effects, integrating $L_{p,s}(x)$ over the range of the middle trainset position during the pass-by duration and summing all sources contributions. It leads to the following expression:

$$\begin{aligned} L_{eq,Tp} &= 10\log\sum_{s\in\mathcal{S}}\frac{1}{L}\int_{-L/2}^{L/2}10^{(L_{p,s}(x)/10}dx \\ &= 10\log\left(\alpha_R 10^{L_H/10}+\alpha_T 10^{L_{W,T}/10}\right) \end{aligned} \tag{4}$$

where $\mathcal{S} = \mathcal{S}_R \cup \mathcal{S}_{Tl} \cup \mathcal{S}_{Th}$ and

$$\begin{aligned} \alpha_R &= \\ &\sum_{s\in\mathcal{S}_R}\frac{1}{L}\int_{-L/2}^{L/2}10^{(L_{r,\mathrm{TOT}}+\Delta L_{W,\mathrm{dir},s}(x)-A_s(x))/10}dx \\ \alpha_T &= \\ &\sum_{s\in\mathcal{S}_{Tl}}\frac{\alpha_l}{n_{Tl}L}\int_{-L/2}^{L/2}10^{(\Delta L_{W,\mathrm{dir},s}(x)-A_s(x))/10}dx \\ &+\sum_{s\in\mathcal{S}_{Th}}\frac{\alpha_h}{n_{Th}L}\int_{-L/2}^{L/2}10^{(\Delta L_{W,\mathrm{dir},s}(x)-A_s(x))/10}dx \end{aligned} \tag{5}$$

For the numerical computation of α_R and α_T, integrals over the vehicle length are discretized using small steps $\delta x = L/5000$.

3.4 Inverse method

For each site, Eq. 4 expresses the relationship between the two quantities to be identified and the equivalent pressure level measured on one single microphone for one single pass-by at a given speed V. It may first be expressed in terms of quadratic pressure $p_{eq}^2 = p_0^2 10^{L_{eq,Tp}/10}$ in order to obtain a linear relationship, more suitable for inversion:

$$p_{eq}^2/p_0^2 = \alpha_R H_R + \alpha_T W_T/W_0 \tag{6}$$

It can then be noted that both parameters $H_R = 10^{L_H/10}$ and $W_T = W_0 10^{L_{W,T}/10}$ are independent of microphone position and vehicle speed. They can thus be identified by combining the N equivalent pressures measured for different microphone positions and pass-by speeds in one global vector $\mathbf{p_{eq}^2}$ leading to the following rectangular linear system:

$$\begin{aligned} \frac{\mathbf{p_{eq}^2}}{p_0^2} &= \left\{\begin{array}{c} p_{eq1}^2/p_0^2 \\ \cdots \\ p_{eqN}^2/p_0^2 \end{array}\right\} \\ &= H_R\left\{\begin{array}{c} \alpha_{R1} \\ \cdots \\ \alpha_{RN} \end{array}\right\} + \frac{W_T}{W_0}\left\{\begin{array}{c} \alpha_{T1} \\ \cdots \\ \alpha_{TN} \end{array}\right\} \\ &= \boldsymbol{\alpha_R} H_R + \boldsymbol{\alpha_T} W_T/W_0 \end{aligned} \tag{7}$$

In addition, as pointed out above, traction noise may be supposed to be independent of the site whereas specific transfer functions for each site have to be identified. A global identification process is thus proposed by combining results from the four sites A to D in one single algebraic system:

$$\left\{\begin{array}{c} \mathbf{p_{eqA}^2}/p_0^2 \\ \mathbf{p_{eqB}^2}/p_0^2 \\ \mathbf{p_{eqC}^2}/p_0^2 \\ \mathbf{p_{eqD}^2}/p_0^2 \end{array}\right\} = [\mathbf{A}]\left\{\begin{array}{c} H_{RA} \\ H_{RB} \\ H_{RC} \\ H_{RD} \\ W_T/W_0 \end{array}\right\} \tag{8}$$

with

$$[\mathbf{A}] = \left[\begin{array}{ccccc} \boldsymbol{\alpha_{RA}} & \mathbf{0} & \mathbf{0} & \mathbf{0} & \boldsymbol{\alpha_{TA}} \\ \mathbf{0} & \boldsymbol{\alpha_{RB}} & \mathbf{0} & \mathbf{0} & \boldsymbol{\alpha_{TB}} \\ \mathbf{0} & \mathbf{0} & \boldsymbol{\alpha_{RC}} & \mathbf{0} & \boldsymbol{\alpha_{TC}} \\ \mathbf{0} & \mathbf{0} & \mathbf{0} & \boldsymbol{\alpha_{RD}} & \boldsymbol{\alpha_{TD}} \end{array}\right] \tag{9}$$

The measurements corresponding to 20 pass-bys in all for the four sites and 2 microphones (lower and upper) per pass-by are used, leading to a 40×5 rectangular system to be inversed. The resolution is performed independently for each third of octave band, by using a constrained least squares optimization. The MATLAB function `lsqlin` is used, allowing the application of bounds to the unknowns, since constraints are necessary to guide the resolution in order to obtain more physical results. For each third of octave band, the following limits are applied:

- transfer functions H_R: the limits are based on the default value of the transfer functions proposed in CNOSSOS-EU corresponding to the closest track/vehicle combination (-20 dB to $+10$ dB with respect to the default transfer function),
- sound powers W_T : the lower limit is arbitrarily set at 60 dB whereas the upper limit is set according to measurements, by imposing that the noise due to traction sources is always lower than the overall noise.

4. RESULTS

Following the method outlined in the previous section, unknown spectra W_T and H are identified from the measure-

ments presented in section 2. Estimations are given respectively in Figs. 6 and 7. They are compared with some default values provided in the CNOSSOS method:

- 4 sound power spectra corresponding to electric motorisation (electric multiple unit and electric locomotive, lower and upper),
- 1 total transfer function built from conventional vehicle and track transfer functions chosen as most representative of the tram configuration studied (wheel with diameter 680 mm / concrete mono-block sleepers + medium stiffness rail-pad).

To interpret these results, the equivalent pressure levels at pass-by are calculated from the estimated parameters for the two positions of microphone. In Figs. 8 and 9, the overall levels obtained in dB(A) are plotted for each site as a function of vehicle speed and compared with the measured levels. The contributions of the sources (traction noise or rolling noise) in the calculated noise levels are also given. Finally, Figs. 10 and 11 show the overall correlation between the measurements and the results obtained with the identified parameters.

4.1 Analysis of the estimated spectra

The traction noise spectrum obtained in Fig. 6 is realistic and compares quite well with CNOSSOS-EU reference spectra in terms of order of magnitude. The spectrum is quite discontinuous with some maxima in certain thirds of octave bands. Actually, outside of these "peaks", levels drop sharply to the limits imposed by the identification method. At these frequencies (100, 200, 1600 and 3150 Hz), it seems that the contribution of traction noise is too small compared to rolling noise to be correctly identified.

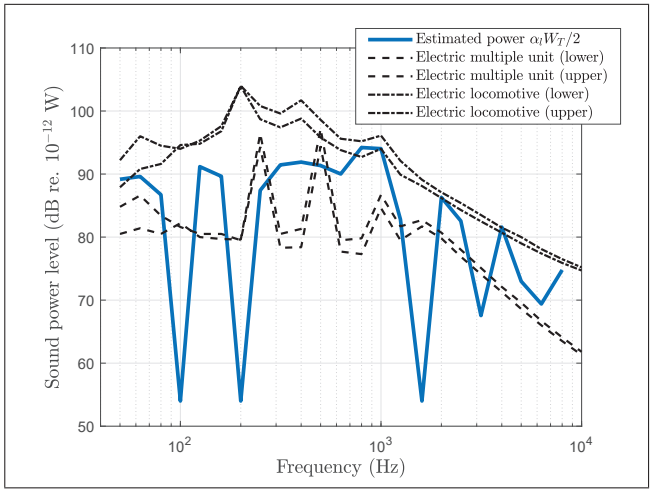

Figure 6. Estimated sound power spectrum corresponding to traction noise (multiplied by $\alpha_l = 0.5$ to keep only the lower=upper part and divided by 2 to obtain a power per coach) and comparison with CNOSSOS-EU spectra.

The estimated transfer functions for sites B and C, given in Fig. 7, are close to the CNOSSOS-EU transfer function but always several dB lower (up to 10 dB in some thirds of octave bands) which is not surprising for the tram. They are also quite close to each other, even though they are more clearly separate above 2000 Hz. For these two sites, the transfer function seems to be well identified, considering that the estimated rolling noise is always above the traction noise (see Figs. 8 and 9 for the global contributions).

The estimated transfer function of site D is similar to that of sites B and C in medium and high frequencies but has much lower values at low frequencies (below 200Hz). In fact, at these frequencies the traction noise has a large contribution to the total noise (even at high speeds) and the identification of the transfer function due to rolling noise is delicate due to the various inaccuracies of the model. The low values obtained at these frequencies are therefore probably not very accurate.

The measurements carried out on site A are special because all the pass-bys are at low speed (less than 25 km/h). Generally speaking, at low speeds, rolling noise is low and traction noise is the main contribution to the total noise. This is confirmed by the estimation of the different contributions for site A in Figs. 8 and 9. This results in a very convincing estimation of the traction noise (see remarks above) but leads to difficulties in calculating a consistent transfer function for this site, due to the various uncertainties. Thus, the transfer function obtained for site A is of limited use.

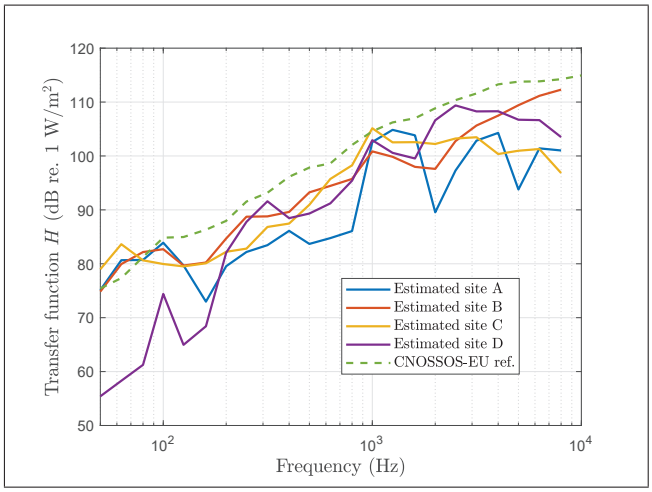

Figure 7. Estimated transfer function corresponding to rolling noise (per axle) and comparison with default CNOSSOS-EU transfer function (default spectra for wheel with diameter 680 mm + concrete mono-block sleepers/medium stiffness rail-pad).

4.2 Variation with vehicle speed

An important characteristic of the noise emission of rail-bound vehicles is the variation with speed of the pressure levels due to rolling noise (in $\alpha \log V$). This variation is generally calculated on the overall pressure levels in dB(A). Slopes α calculated from the equivalent noise levels obtained with the estimated parameters, on each site

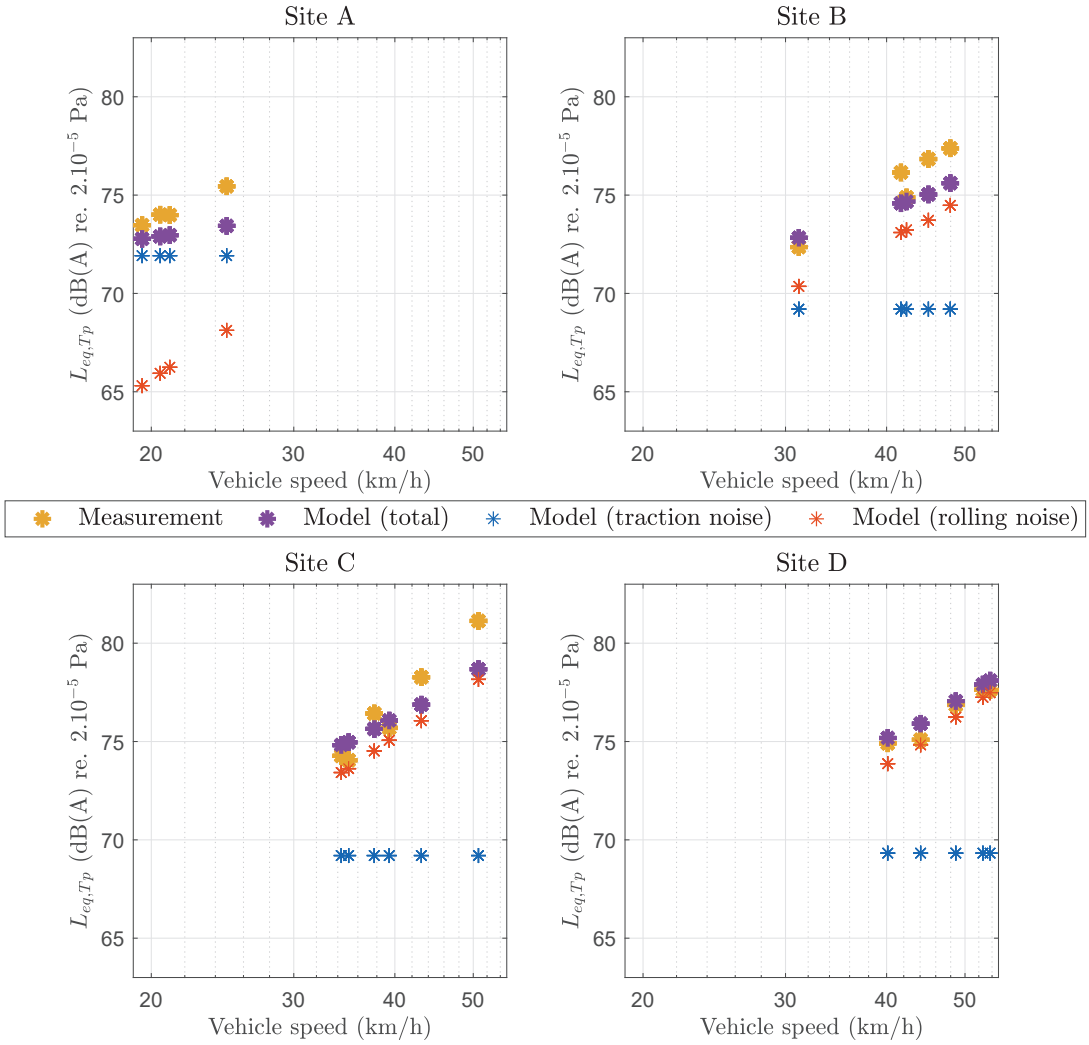

Figure 8. Measured and calculated equivalent noise levels at pass-by on the lower microphone as a function of vehicle speed, with estimated contributions of traction noise and rolling noise

and for each microphone, are presented in Tab. 1. In general, the slopes obtained from measurement or modelling for conventional rail vehicles running on ballasted tracks are around 30. This rule is rather well respected on site D, whose track is closest to a conventional ballasted track. On the other sites the α values remain within realistic limits.

Microphone/Site	A	B	C	D
Lower	25.0	21.6	27.8	29.2
Upper	26.4	25.9	33.4	30.1

Table 1. Slopes α of variations with speed for estimated rolling noise.

4.3 Global errors

Finally, in Figs 10 and 11, the correlations between the measured noise levels and the noise levels calculated from the identified parameters show that the differences are contained between -2 and +2 dB approximately for the lower microphone and between -1.5 and +1.5 dB approximately for the upper microphone. These results are rather satisfactory considering the very rough assumption that there is no variation of the traction noise. Indeed, a detailed frequency band analysis (not shown here) shows that the amplitudes of the traction noise peaks can change significantly with speed. Thus, the identification process tends to assimilate a fraction of these peaks to rolling noise because of the variation with speed.

5. CONCLUSIONS

Within the framework of the production of noise maps to comply with European Directive 2002/49/EC relating to the assessment and management of environmental noise, the aim of this work was to empirically determine the emission parameters of some trams of the Lyon network, in ac-

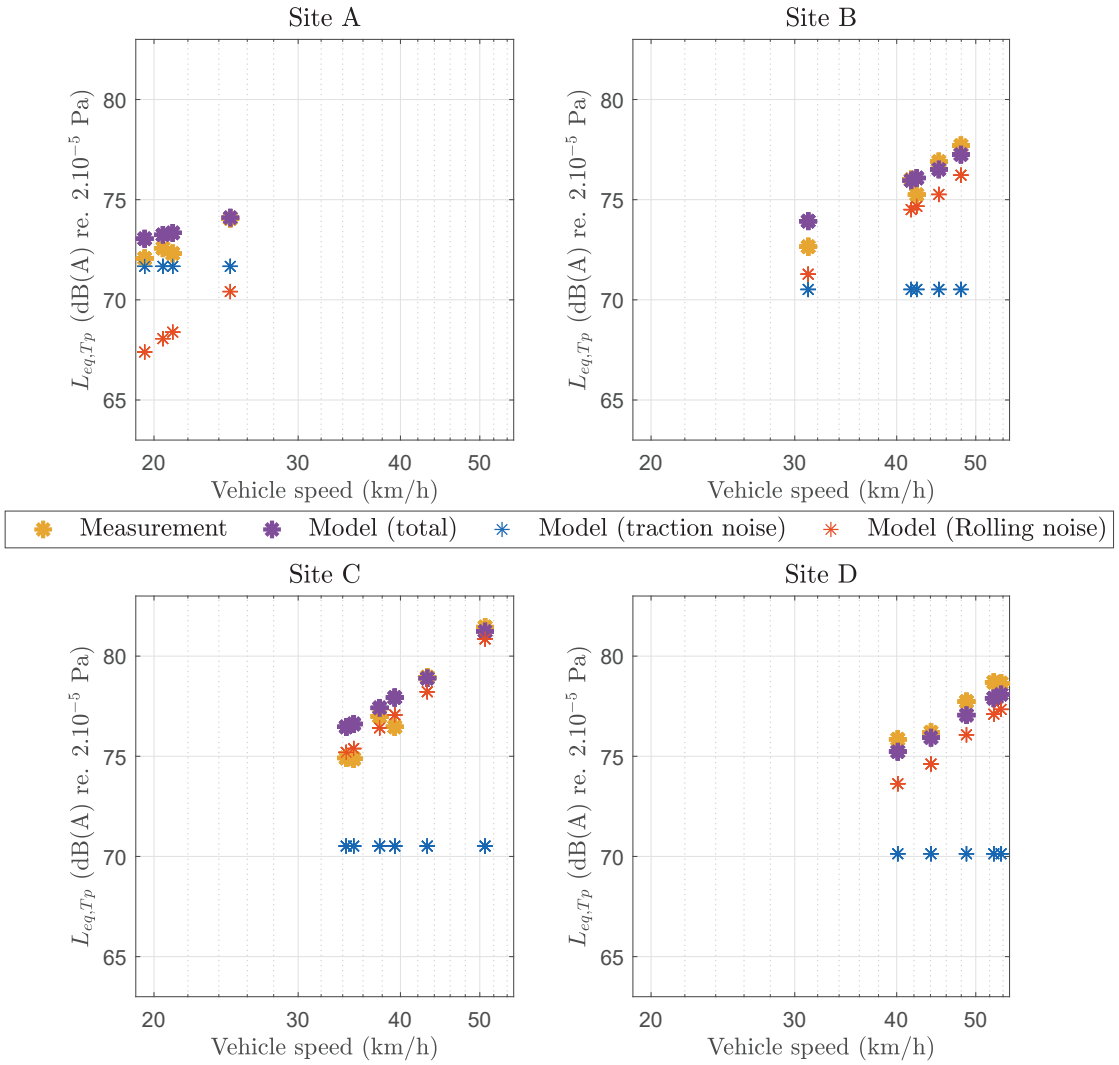

Figure 9. Measured and calculated equivalent noise levels at pass-by on the upper microphone as a function of vehicle speed, with estimated contributions of traction noise and rolling noise .

cordance with the new CNOSSOS-EU method. The parameters sought are the power spectrum of traction noise sources and the total transfer function (vehicle + track) relating to rolling noise. These parameters are determined on the basis of a series of measurements carried out on site: pass-by noise levels according to standard ISO 3095 and wheel/rail roughness measurements according to standard EN 15610. The identification method is based on the inversion of specific emission and propagation models adapted to the assessment of equivalent pass-by noise levels. A global identification process is proposed by combining results from sites with different tracks (rail, supports and surfacing), pass-bys at various speeds and two microphones. Results are satisfactory for a first study. The separation of traction noise and rolling noise seems possible and leads to realistic spectra.

Further work is in progress in order to increase the performance of the method. Results of some vibro-acoustic models of tram tracks combined with track decay rates (TDR) measurements on site will notably be used in order to separate the track and vehicle contributions to rolling noise in the transfer function.

6. ACKNOWLEDGEMENTS

This work was supported by the LabEx CeLyA (ANR-10-LABX-0060) of Université de Lyon, within the program "Investissements d'Avenir" (ANR-11-IDEX-0007) operated by the French National Research Agency (ANR).

We would also like to thank the association Acoucité "Soundscape and noise observatory of Greater Lyon", for providing the results of the acoustic experimental campaign on the Lyon tram network.

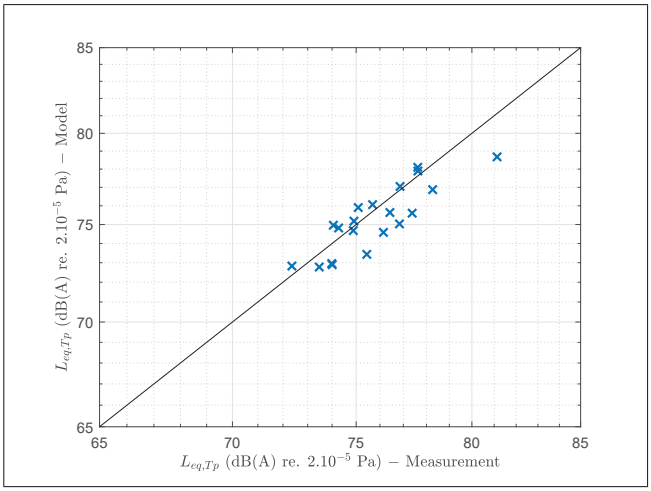

Figure 10. Correlations between measured and calculated equivalent noise levels at pass-by on the lower microphone.

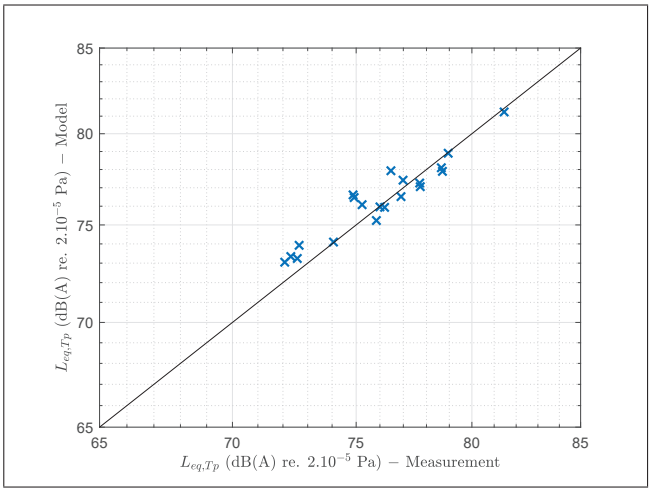

Figure 11. Measured and calculated equivalent noise levels at pass-by on the upper microphone.

7. REFERENCES

[1] Directive 2002/49/EC of the European Parliament and of the Council of 25 June 2002 relating to the assessment and management of environmental noise, July 2002.

[2] Commission Directive (EU) 2015/996 of 19 May 2015 establishing common noise assessment methods according to Directive 2002/49/EC of the European Parliament and of the Council, July 2015.

[3] S. L. Grassie, "Rail irregularities, corrugation and acoustic roughness: characteristics, significance and effects of reprofiling," *Proceedings of the Institution of Mechanical Engineers, Part F: Journal of Rail and Rapid Transit*, May 2012.

[4] L. Chiacchiari and G. Loprencipe, "Measurement methods and analysis tools for rail irregularities: a case study for urban tram track," *Journal of Modern Transportation*, vol. 23, pp. 137–147, June 2015.

[5] L. Chiacchiari, D. J. Thompson, G. Squicciarini, E. Ntotsios, and G. Loprencipe, "Rail roughness and rolling noise in tramways," *Journal of Physics: Conference Series*, vol. 744, p. 012147, Sept. 2016.

[6] Y. Zhao, X. Li, Q. Lv, H. Jiao, X. Xiao, and X. Jin, "Measuring, modelling and optimising an embedded rail track," *Applied Acoustics*, vol. 116, pp. 70–81, Jan. 2017.

[7] O. Chiello, A. Le Bellec, M.-A. Pallas, P. Muñoz, and V. Janillon, "Characterisation of wheel/rail roughness and track decay rates on a tram network," in *Proceeding of Inter-Noise 2019*, (Madrid, Spain), June 2019.

[8] Y. K. Wijnia, "Noise emission from trams," *Journal of Sound and Vibration*, vol. 120, pp. 281–286, Jan. 1988.

[9] J. Mandula, B. Salaiová, and M. Koval'aková, "Prediction of noise from trams," *Applied Acoustics*, vol. 63, pp. 373–389, Apr. 2002.

[10] M. A. Pallas, J. Lelong, and R. Chatagnon, "Characterisation of tram noise emission and contribution of the noise sources," *Applied Acoustics*, vol. 72, pp. 437–450, June 2011.

[11] E. Panulinová, "Input Data for Tram Noise Analysis," *Procedia Engineering*, vol. 190, pp. 371–376, Jan. 2017.

[12] S. Van Lier, "The vibro-acoustic modelling of slab track with embedded rails," *Journal of Sound and Vibration*, vol. 231, pp. 805–817, Mar. 2000.

[13] C. M. Nilsson, C. J. C. Jones, D. J. Thompson, and J. Ryue, "A waveguide finite element and boundary element approach to calculating the sound radiated by railway and tram rails," *Journal of Sound and Vibration*, vol. 321, pp. 813–836, Apr. 2009.

[14] W. Sun, D. Thompson, M. Toward, M. Wiseman, E. Ntotsios, and S. Byrne, "The influence of track design on the rolling noise from trams," *Applied Acoustics*, vol. 170, p. 107536, Dec. 2020.

[15] W. Sun, D. Thompson, M. Toward, and Z. Zeng, "Modelling of vibration and noise behaviour of embedded tram tracks using a wavenumber domain method," *Journal of Sound and Vibration*, vol. 481, p. 115446, Sept. 2020.

[16] M. C. Bérengier, B. Gauvreau, P. Blanc-Benon, and D. Juvé, "Outdoor Sound Propagation: A Short Review on Analytical and Numerical Approaches," *Acta Acustica united with Acustica*, vol. 89, pp. 980–991, Nov. 2003.

[17] M. E. Delany and E. N. Bazley, "Acoustical properties of fibrous absorbent materials," *Applied Acoustics*, vol. 3, pp. 105–116, Apr. 1970.